

Approximations for Implicitly-Defined Dynamics of Networks of Simple Mechanical Components

Bill Goodwine

Abstract—In many important engineering systems, including cyber-physical systems, there are often many interacting simple components. It is well known that, in some cases, such systems may be modeled with fractional-order differential equations, and some of our prior work has shown that in certain cases fractional systems may be considered a subset of a class of systems where the dynamics may only be implicitly defined. In the implicit case, there is no straight-forward corresponding time domain representation. This paper considers series expansion approximations to the implicit operator describing the dynamics of the system to determine time-domain approximations for the implicit non-rational transfer function and validates the results via simulation. The contribution of this paper is to show that such expansions provide good approximations for the types of systems in the range of parameter values we considered, and for the special case of a network of springs and dampers, accurate equivalent spring and damper constants are computed which can provide intuitive insight into the nature of the response of the very high-order system.

I. INTRODUCTION

Consider the system illustrated in Figures 1 and 2, which is a network of masses, springs and dampers. Alternatively, this can be considered as a formation of robots where each robot controls its position based on its position relative to its neighbors in accordance with a spring and damper-like control force. Even more generally, this may be considered a network of interacting components where the dynamics of the interactions between two components are described by operators, G_1 and G_2 , with springs and dampers being specific examples, *i.e.*, $G_1(s) = k$ and $G_2(s) = bs$, where s is the usual derivative operator. In this case, the operator takes the relative displacements of elements and returns the force generated by the network between them. It will be clear in this paper that the results are not limited to spring and damper interactions, but for clarity of presentation, this paper will generally focus on those as specific examples.

A. Fractional and Implicit Systems

The network in Figure 1 can be considered as a graph where each node is a mass and each edge is either a spring or damper. For the system illustrated, the graph representing the network is a tree where each subsequent generation (to the right) contains three nodes connected to each node where two of the edges are springs and one is a damper. We consider generalizations to this network where there are n springs and m dampers connected to each subsequent generation,

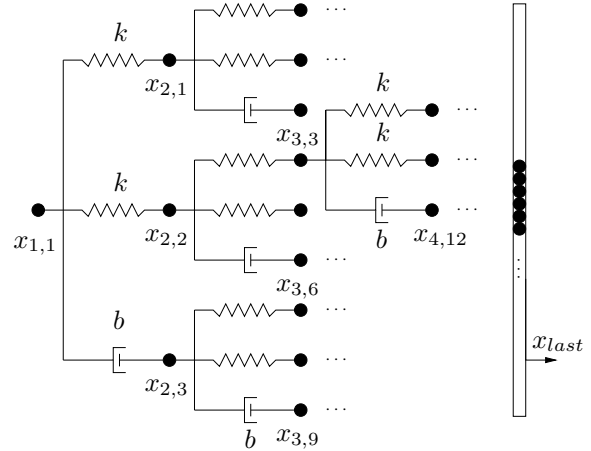


Fig. 1. Model of networked system where each node is a mass and $x_{i,j}$ denotes the position of mass j in generation i of the network.

as illustrated in Figure 2, or more generally, n edges with operator G_1 and m edges with operator G_2 .

Denote by G_∞ the operator representing the relationship between $x_{1,1}$ and x_{last} , *i.e.*, spanning the entire network. In the mechanical case, G_∞ represents the force on the right-most node as a function of the relative position of x_{last} with respect to $x_{1,1}$, *i.e.*, the dynamics of x_{last} are described by

$$m_{last}s^2X_{last}(s) = G_\infty(s)(X_{1,1}(s) - X_{last}(s)),$$

where $X_{i,j}(s)$ is the Laplace transform of $x_{i,j}(t)$. This paper considers cases where the network is *self-similar*, meaning that it is large enough such that the operator describing the force on the last node is the same from any node to the last node. This will happen in cases where the network has a large number of generations.

In the special case where $n = 1$ and $m = 1$ and the masses at the internal nodes are negligible, it is well-known that the system is described by a *fractional-order differential equation* and $G_\infty(s) = \sqrt{kb}\sqrt{s}$. In [1] we showed that, in the context of robotic formation control, the corresponding time-domain differential equation containing the half-order derivative matches the dynamics of the very large scale system with a concise fractional-order representation.

However, any other combination of n and m does *not* lead directly to a fractional-order representation, but rather to a non-fractional order irrational operator. In [2] we employed a fractional-order system identification procedure to determine fractional-order approximations to these systems. In contrast, this paper considers *integer-order series expansions* for these operators to determine time-domain representations.

Department of Aerospace & Mechanical Engineering,
University of Notre Dame, Notre Dame, IN 46556 USA,
bill@controls.ame.nd.edu.

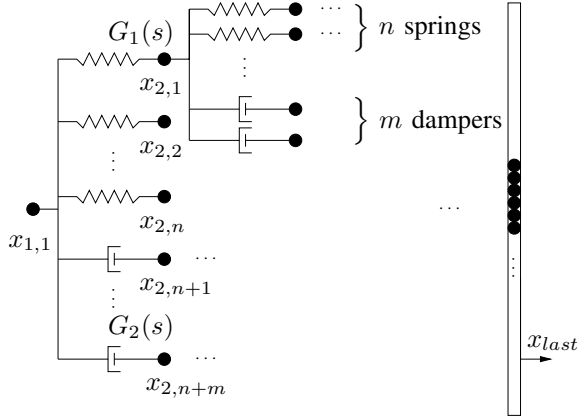


Fig. 2. Model of a more general networked system.

B. Literature Review

Control of multi-robot systems has been very topical for many years [3]–[7], with much effort considering how to make representations of very large systems tractable and concise enough to be useful in design and control. Some previous work by the author has been along these lines by considering *exact* model reduction for systems with symmetries [8]–[11].

Fractional calculus has a long history back to near the beginning of calculus and books on the mathematics of fractional calculus and engineering applications include [12]–[14], and there are some review articles such as [15], [16]. The system in Figure 1 was originally developed as a viscoelastic model from [17], [18]. The work in [19], [20], concerns formation control of fractional systems; however, the components within the system are individually fractional. In this paper, in contrast, the fractional dynamics arise from the structure of the agents' interactions and are a feature of the collective dynamics of the system. Other papers from the authors on fractional calculus in engineering are [21], [22].

C. Self-Similarity in Networked Systems

Consider the nature of the operator that relates the relative displacement of the first and last generations to the force generated by the network. In the limit as the number of generations goes to infinity, the system is characterized by a *self-similarity*; specifically, with an infinite number of generations, the transfer function between $x_{1,1}$ and x_{last} is equal to the transfer function between any other x_{ij} to x_{last} .

In the spring and damper case $G_1(s) = k$ and $G_2(s) = bs$, where k and b are the spring and damper coefficients. For the moment, if we consider the case where there is only one spring and one damper between each generation, i.e., $n = m = 1$ in Figure 2, then the usual parallel ($G = G_1 + G_2$) and series ($G = 1/(1/G_1 + 1/G_2)$) rules for interconnected

mechanical components gives

$$\begin{aligned} G_\infty(s) &= \frac{1}{\frac{1}{G_1(s)} + \frac{1}{G_\infty(s)}} + \frac{1}{\frac{1}{G_2(s)} + \frac{1}{G_\infty(s)}} \\ &= \frac{G_1(s)G_\infty(s)}{G_1(s) + G_\infty(s)} + \frac{G_2(s)G_\infty(s)}{G_2(s) + G_\infty(s)}. \end{aligned}$$

The algebra is straight-forward, but many terms cancel in this case which do not in other cases, so we show the steps here. Cross-multiplying gives

$$\begin{aligned} G_\infty(G_1 + G_\infty)(G_2 + G_\infty) \\ = G_1G_\infty(G_2 + G_\infty) + G_2G_\infty(G_1 + G_\infty) \end{aligned}$$

all of which simplifies to

$$G_\infty^2(s) = G_1(s)G_2(s) \quad \text{or} \quad G_\infty(s) = \sqrt{G_1(s)G_2(s)},$$

the fractional representation for $G_1(s) = k$ and $G_2(s) = bs$ where $G_\infty(s) = \sqrt{kbs}$. The square root of s indicates 1/2-order dynamics and our work in [1] validates this. Only the positive solution is kept if the spring and damper constants represent physical components where they must be positive.

In contrast, now consider the system in Figure 1 where there are two springs and one damper between components in subsequent generation. In this case self-similarity gives

$$G_\infty(s) = \frac{2}{\frac{1}{G_1(s)} + \frac{1}{G_\infty(s)}} + \frac{1}{\frac{1}{G_2(s)} + \frac{1}{G_\infty(s)}}$$

which simplifies to

$$G_\infty^2(s) - G_1(s)G_\infty(s) - 2G_1(s)G_2(s) = 0. \quad (1)$$

This is quadratic in the unknown, $G_\infty(s)$ with known operator coefficients, $G_1(s)$ and $G_2(s)$. The quadratic equation gives an expression for $G_\infty(s)$, but it can not be expressed in the time domain by a fractional- or integer-order time derivative. As such, we must resort to approximations, which are developed in subsequent sections.

II. FREQUENCY-RESPONSE COMPARISON FOR IRRATIONAL REPRESENTATION

This section considers self-similar systems like the one illustrated in Figure 2. We generalize the type of system by considering a system where there are n springs and m dampers on each generation, where Figure 1 illustrates the specific case where $n = 2$ and $m = 1$. In general

$$G_\infty(s) = \frac{n}{\frac{1}{G_1(s)} + \frac{1}{G_\infty(s)}} + \frac{m}{\frac{1}{G_2(s)} + \frac{1}{G_\infty(s)}},$$

which gives the following expression for $G_\infty(s)$

$$\begin{aligned} G_\infty^2(s) - [(n-1)G_1(s) + (m-1)G_2(s)]G_\infty(s) \\ - (n+m-1)G_1(s)G_2(s) = 0. \quad (2) \end{aligned}$$

As before, $G_\infty(s)$ is the transfer function relating the relative displacement of the two ends of the network to the force required for the displacement. This equation for $G_\infty(s)$ has

operator coefficients, which can be formally solved using the quadratic equation to give

$$G_{\infty}(s) = \frac{1}{2} \left[(n-1)G_1(s) + (m-1)G_2(s) \pm \left([(n-1)G_1(s) + (m-1)G_2(s)]^2 + 4(n+m-1)G_1(s)G_2(s) \right)^{1/2} \right]. \quad (3)$$

Because there is no corresponding time domain differential operator for this solution, this paper investigates the efficacy of a series expansion of this solution about $s = 0$. Specifically, a series expansion for $G_{\infty}(s)$ about $s = 0$ is

$$G_{\infty}(s) = (n-1)k + \frac{nmb}{n-1}s - \frac{nm(n+m-1)b^2}{(n-1)^3k}s^2 + \dots \quad (4)$$

Obviously convergence must be considered when relying upon a series expansion such as this. Note that in the operator theory as developed by Mikusiński [23], [24], develops the needed induced topology on the space of operators in which to rigorously consider convergence. In this paper, convergence is verified via simulation of the interested cases; however, it does remain a subject of future work to determine the cases in which convergence is guaranteed.

Before we determine time-domain approximations for this operator, we compare the frequency-response characteristics for a large, but finite, network with the irrational expression for $G_{\infty}(s)$ given by Equation 3. The transfer function from the force to the corresponding displacement will be $1/G_{\infty}(s)$. Figure 3 compares the frequency response of a finite, 3-generation network with $n = 2$, $m = 3$, $k = 2$, $b = 1/10$ and all the internal masses negligible (blue curve) with the infinite approximation given by the irrational solution to the quadratic equation in Equation 3 (red curve). They match nearly exactly for all frequencies. Figure 4 compares the infinite case to the finite, 10-generation case with the same parameter values and the same masses as the previous plot. Note that the finite system has 12, 207, 031 nodes, *i.e.*, is of order $\mathcal{O}(10^7)$, and therefore should be well-modeled by an infinite approximation, as it is because it match is even closer than for the three-generation case.

III. SERIES APPROXIMATIONS

Now compare the frequency response characteristics for the finite, large-scale system and the series approximation to the infinite approximation given by Equation 4. Figure 5 illustrates the frequency-response of the series approximation for one, two and three terms for the same parameter values and number of generations as Figure 4. Clearly there is a good match in the first case for low frequencies up to approximately $\omega \approx 2$ [rad/s], but the series approximation frequency responses diverges from the finite system for larger frequencies. Also, the higher-order approximations appear to be worse than the lower order ones. However, note that this is to be expected for high frequencies. Figure 6 illustrates the same frequency response for frequencies below $\omega = 1$, which does show the expected case that the higher-order series approximations are closer to the real solution.

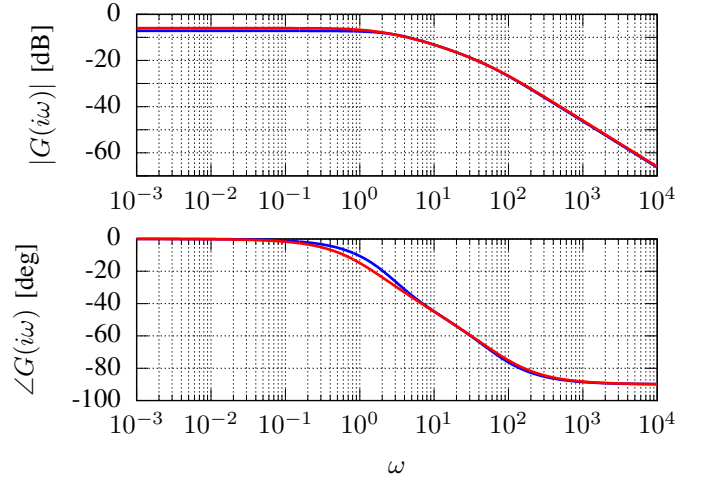


Fig. 3. Frequency response for finite system (blue curve) with irrational infinite-order approximation (red curve) given by Equation 3. For the finite system, there are 3 generations, $n = 2$, $m = 3$, $k = 2$, $b = 1/10$ and the interior masses are negligible.

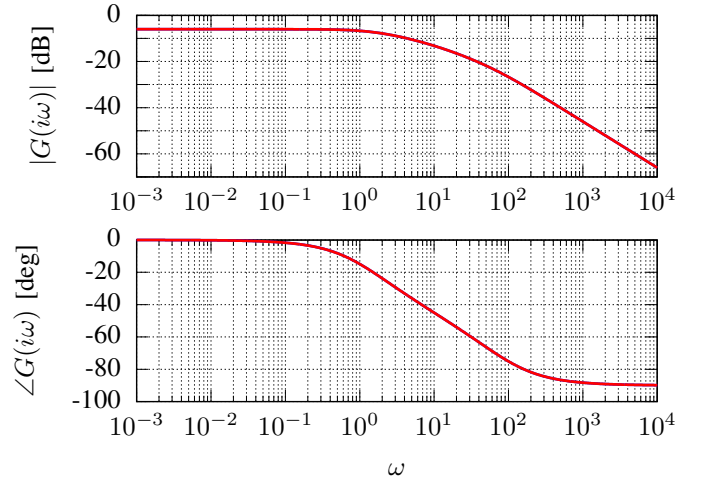


Fig. 4. Frequency response for finite system (blue curve) with irrational infinite-order approximation (red curve) given by Equation 3. For the finite system, there are 10 generations, $n = 2$, $m = 3$, $k = 2$, $b = 1/10$ and the interior masses are negligible. The blue curve is not visible because it matches exactly with the red curve.

Note that in the series expansion in Equation 4, the denominators grow with increased k values and increased numbers of springs, n . As such, better convergence is expected in spring-dominated networks. Figure 7 compares the frequency response of the series approximations with the real system in the case with $n = 2$, $m = 1$, $k = 2$, $b = 1$ and 10 generations. Figure 8 considers a much more spring-dominated system, and compares the frequency response of the series approximations with the real system in the case with $n = 5$, $m = 2$, $k = 2$, $b = 1/10$ and 10 generations, and shows a much better match.

IV. TIME DOMAIN COMPARISON

In the special case where $n = 1$ and $m = 1$, we can compare the time domain response of the finite system with the fractional-order time domain solution. Consider the

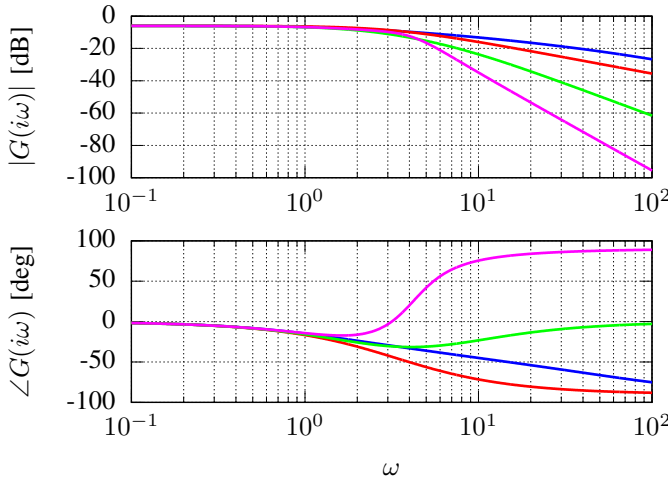


Fig. 5. Frequency response for finite system (blue curve) with series approximations to the infinite-order solution given by Equation 4. For the finite system, there are 10 generations, $n = 2$, $m = 3$, $k = 2$, $b = 1/10$, the mass of the last generation is one and the interior masses are negligible. Blue: actual system. Red: first-order approximation. Green: second-order approximation. Magenta third-order approximation.

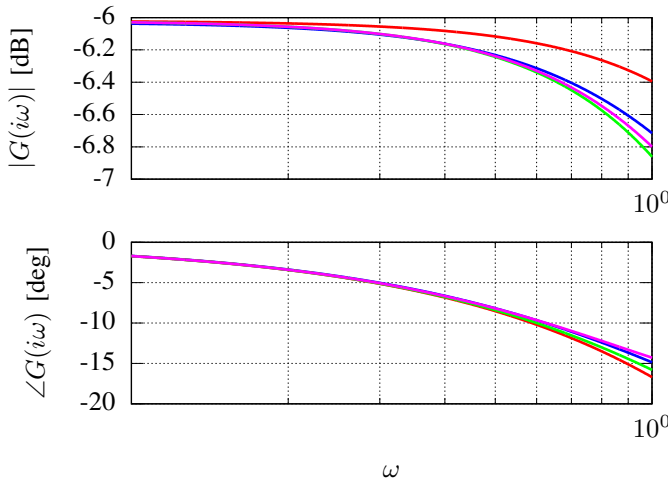


Fig. 6. Same frequency response as plotted in Figure 5, but zoomed in to lower frequency range. Blue: actual system. Red: first-order approximation. Green: second-order approximation. Magenta third-order approximation.

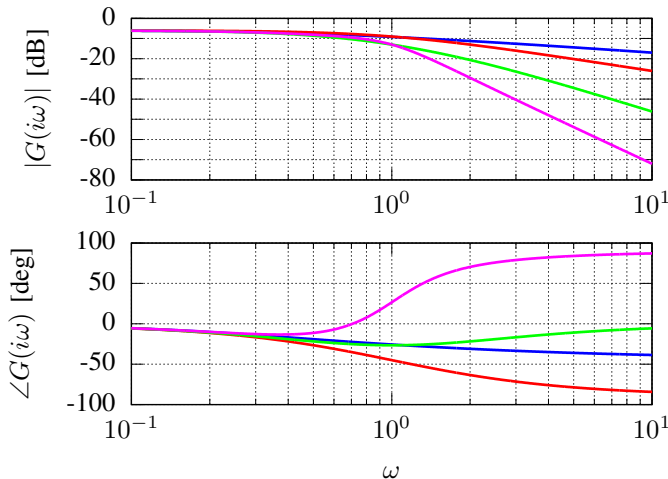


Fig. 7. Frequency response for a system with significant damping.

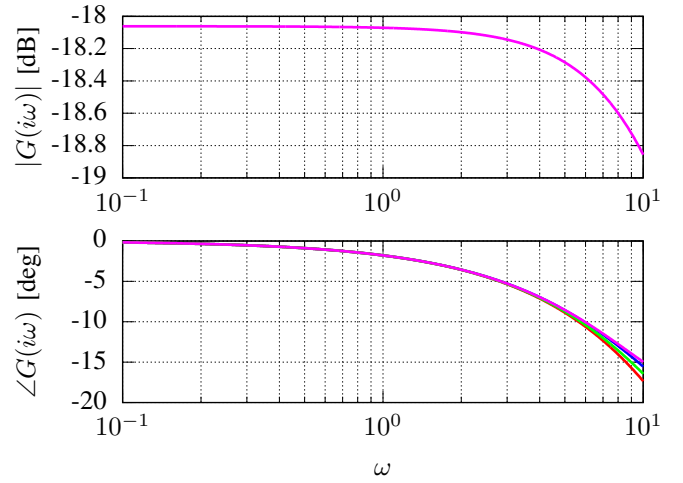


Fig. 8. Frequency-response of a spring-dominated network, showing better convergence of series approximations.

motion of x_{last} to a step-input type change in the left-most mass given by

$$x_{1,1}(t) = \frac{1}{1 + e^{-\alpha(t-1)}}$$

with $\alpha = 8$. If $x_{1,1}(t)$ is taken as indicated above and considered the input to the system, then the motion of the last generation is given by the solution to

$$m_{last} \frac{d^2 x_{last}}{dt^2}(t) + \sqrt{kb} \frac{d^{1/2} x_{last}}{dt^{1/2}}(t) = \sqrt{kb} \frac{d^{1/2} x_{1,1}}{dt^{1/2}}(t).$$

The fractional solution illustrated in Figure 9 was computed numerically using the Grünwald Letnikov derivative,

$$\frac{d^\alpha x}{dt^\alpha}(m\Delta t) \approx \frac{\sum_{0 \leq n \leq m} (-1)^n \frac{\Gamma(\alpha+1)}{\Gamma(n+1)\Gamma(\alpha-n+1)} x(t + (\alpha - n)\Delta t)}{(\Delta t)^\alpha}$$

with $\Delta t = 0.005$, $k = 1$, $b = 1/3$. With seven generations, the fractional and exact solutions are nearly identical, as illustrated in Figure 9. See [1] for a more complete exposition.

Unfortunately, for all the other cases where both n and m are not equal to one, there is no exact corresponding time domain fractional derivative representation for the system, motivating the use of the integer-order series approximation to Equation 3 and the corresponding time-domain integer-order derivative representation to compute a solution.

Still taking $x_{1,1}(t)$ as an input, the corresponding time-domain differential equation for $x_{last}(t)$ using the series approximation and including through the first order term is

$$\ddot{x}_{last}(t) = (n-1)k(x_{1,1}(t) - x_{last}(t)) + \frac{nm}{n-1}b(\dot{x}_{1,1}(t) - \dot{x}_{last}(t)). \quad (5)$$

The interpretation of this is that there are equivalent stiffness, damping and mass terms from the series expansion. Specifically,

$$k_{eq} = (n-1)k, \quad b_{eq} = \frac{nm}{n-1}b.$$

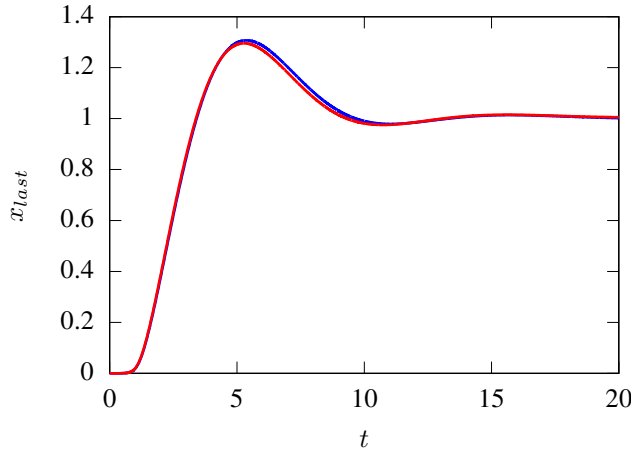


Fig. 9. Comparison of exact solution for system with seven generations, $k = 1$, $b = 1/3$ and seven generations to the 1/2-order fractional derivative representation of the transfer function.

Naturally the equivalent spring and damper terms are proportional to k and b respectively and increase as the corresponding number of each increases with each generation. Interestingly, the equivalent damping is function of the number of springs, but the equivalent spring constant is not a function of the number of dampers. There is also a “subtracted mass” effect if the series is used through the second-order term in Equation 4.

Figure 10 compares the full solutions for three generations, $n = 4$, $m = 1$, $k = 2$ and $b = 1/10$ with the series approximation including through the first-order term in Equation 5. Figure 11 compares the full solutions for three generations, $n = 2$, $m = 1$, $k = 2$ and $b = 1/10$ with the same series approximation. In each case, the series solution provides a good approximation to the full solution. The natural frequency is increased in the $n = 4$ case relative to $n = 2$. Finally, because of the $(n - 1)^3$ term in the denominator of the second-order term in the series, when n is decreased, the approximate solution though first order becomes less accurate, as is apparent in Figure 11 compared with Figure 10.

A benefit to the series approximation is that it provides a low-order and concise description of the system. For the computations needed for Figures 10 and 11, the full solution took approximately 100 times longer to compute using the octave `lsode()` routine than the approximate solution. Furthermore, the coefficients in the series expansion gives readily interpretable insight into the effect of changing parameters in the system to the response of the system.

Figures 12 and 13 illustrate the nature of the change in the response of the system and the accuracy of the series approximately as m is changed. Figure 12 was for the same k and b values as previously, but for $n = 3$ and $m = 1$. Figure 13 was the same except $m = 3$ (more dampers), with a clear effect on the response. Note, that unlike changing the number of springs, altering the number of dampers does not significantly alter the accuracy of the series solution.

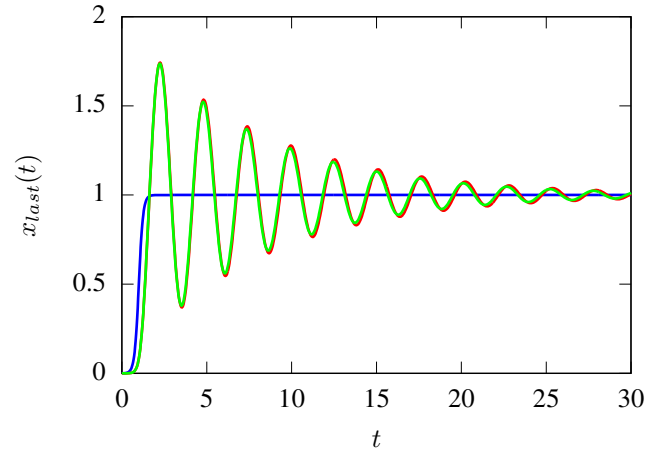


Fig. 10. Comparison of series solution with actual solution with three generations, $n = 4$, $m = 1$, $k = 2$ and $b = 1/10$. The blue curve is the displacement of the first mass. The red curve is the solution of the full system. The green curve is the solution to the series approximation in Equation 5.

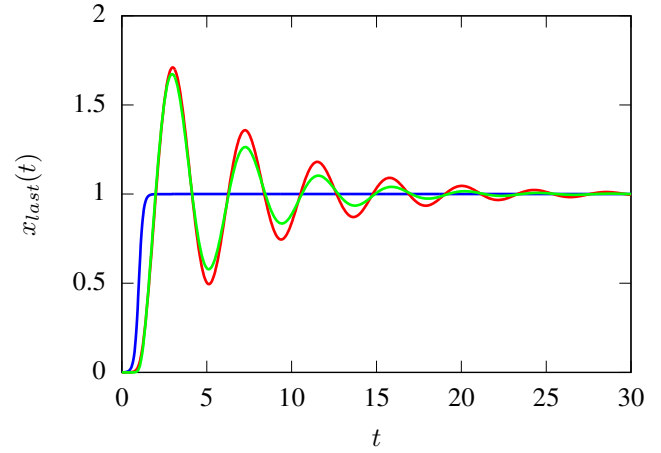


Fig. 11. Comparison of series solution with actual solution with three generations, $n = 2$, $m = 1$, $k = 2$ and $b = 1/10$. The blue curve is the displacement of the first mass. The red curve is the solution of the full system. The green curve is the solution to the series approximation in Equation 5.

V. CONCLUSIONS AND FUTURE WORK

This paper considered the dynamics of tree-like networks of mechanical components. In particular, in the limit of an infinite number of generations, is characterized by self-similarity. Only in one case, one spring and one damper added at each generation, can the relationship between the displacement of the network and its force be expressed in a form that has a time domain linear operator expressions (a pure fractional derivative). When we consider different combinations with more springs or dampers, we can not determine a time domain representation that is exactly a fractional- or integer-order derivative. This paper considered a series expansion of the irrational transfer function that arises from the self-similarity and interpreted the coefficients in the expansion relative equivalent second-order system

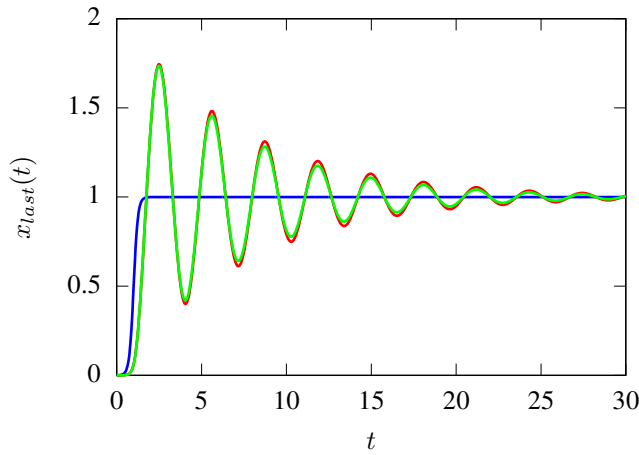


Fig. 12. Comparison of series solution with actual solution with three generations, $n = 3$, $m = 1$, $k = 2$ and $b = 1/10$. The blue curve is the displacement of the first mass. The red curve is the solution of the full system. The green curve is the solution to the series approximation in Equation 5.

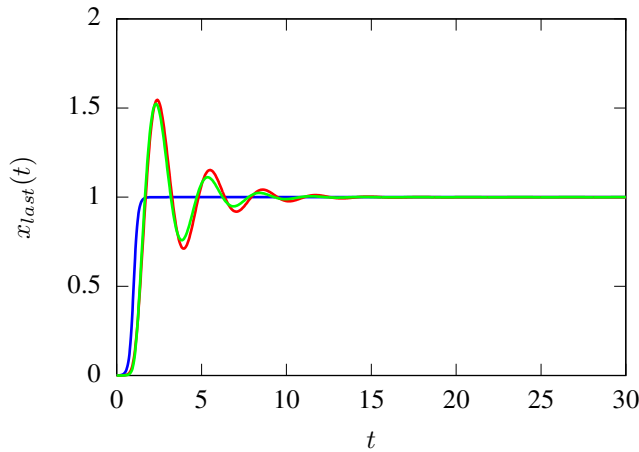


Fig. 13. Comparison of series solution with actual solution with three generations, $n = 3$, $m = 3$, $k = 2$ and $b = 1/10$. Note the obvious effect of increased damping, but less change in the accuracy of the series compared with the case where n was changed (Figures 10 and 11). The blue curve is the displacement of the first mass. The red curve is the solution of the full system. The green curve is the solution to the series approximation in Equation 5.

spring and damper constants. The series converges faster, and hence is more accurate, as the number of springs is increased. The number of springs also affects the equivalent damping; whereas, the number of dampers does not affect the equivalent stiffness.

ACKNOWLEDGMENT

The author would like to thank Mihir Sen, Kevin Leyden and Fabio Semperlotti for many interesting and helpful conversations related to the subject matter of this paper.

REFERENCES

[1] Bill Goodwine. Modeling a multi-robot system with fractional-order differential equations. In *Proceedings of the IEEE International Conference on Robotics and Automation*, pages 1763–1768, 2014.

[2] Bill Goodwine. Fractional-order approximations to implicitly-defined operators for modeling and control of networked mechanical systems. In *Proceedings of the IEEE International Symposium on Intelligent Control (ISIC)*, pages 1–7, Buenos Aires, Argentina, 2016.

[3] Wei Ren, Randal W. Beard, and Ella M. Atkins. Information consensus in multivehicle cooperative control. *IEEE Control Systems Magazine*, pages 71–82, April 2007.

[4] J. Alexander Fax and Richard M. Murray. Information flow and cooperative control of vehicle formations. *IEEE Transactions on Automatic Control*, 49(9):1465–1476, 2004.

[5] Aveek K. Das, Rafael Fierro, Vijay Kumar, James P. Ostrowski, John Spletzer, and Camillo J. Taylor. A vision-based formation control framework. *IEEE Transactions on Robotics and Automation*, 18(5):813–825, 2002.

[6] Richard M Murray. Recent research in cooperative control of multivehicle systems. *Journal of Dynamic Systems Measurement and Control*, 129(5):571, 2007.

[7] Yongcan Cao, Wenwu Yu, Wei Ren, and Guanrong Chen. An overview of recent progress in the study of distributed multi-agent coordination. *Industrial Informatics, IEEE Transactions on*, 9(1):427–438, 2013.

[8] M. Brett McMickell and Bill Goodwine. Reduction and non-linear controllability of symmetric distributed systems. *International Journal of Control*, 76(18):1809–1822, 2003.

[9] M. Brett McMickell and Bill Goodwine. Motion planning for nonlinear symmetric distributed robotic formations. *The International journal of robotics research*, 26(10):1025–1041, 2007.

[10] Bill Goodwine and Panos J. Antsaklis. Multi-agent compositional stability exploiting system symmetries. *Automatica*, pages 3158–3166, 2013.

[11] M. Brett McMickell and Bill Goodwine. Reduction and non-linear controllability of symmetric distributed systems with drift. In *Proceedings of the IEEE International Conference on Robotics and Automation*, pages 3454–3460, 2002.

[12] Keith B. Oldham and Jerome Spanier. *The Fractional Calculus*. Academic Press, New York, 1974.

[13] Dumitru Baleanu, José António Tenreiro Machado, and Albert C. J. Luo. *Fractional Dynamics and Control*. Springer Publishing Company, Incorporated, 2011.

[14] Manuel Duarte Ortigueira. *Fractional Calculus for Scientists and Engineers*, volume 84 of *Lecture Notes in Electrical Engineering*. Springer, 2011.

[15] M.D. Ortigueira. An introduction to the fractional continuous-time linear systems: the 21st century systems. *Circuits and Systems Magazine, IEEE*, 8(3):19–26, 2008.

[16] J. Tenreiro Machado, Virginia Kiryakova, and Francesco Mainardi. Recent history of fractional calculus. *Communications in Nonlinear Science and Numerical Simulation*, 16(3):1140 – 1153, 2011.

[17] N. Heymans and J.C. Bauwens. Fractal rheological models and fractional differential equations for viscoelastic behavior. *Rheologica Acta*, 33:210219, 1994.

[18] Jason Mayes. *Reduction and Approximation in Large and Infinite Potential-Driven Flow Networks*. PhD thesis, University of Notre Dame, 2012.

[19] Yongcan Cao and Wei Ren. Distributed formation control for fractional-order systems: Dynamic interaction and absolute/relative damping. *Systems & Control Letters*, 59(34):233 – 240, 2010.

[20] Yongcan Cao, Yan Li, Wei Ren, and Yang Quan Chen. Distributed co-ordination of networked fractional-order systems. *Systems, Man, and Cybernetics, Part B: Cybernetics, IEEE Transactions on*, 40(2):362–370, 2010.

[21] Bill Goodwine. Fractional-order dynamics in a random, approximately scale-free network of agents. In *Proceedings of the IEEE Conference on Control Automation Robotics & Vision*, pages 1581–1586, 2014.

[22] Bill Goodwine and Kevin Leyden. Recent results in fractional-order modeling for multi-agent systems and linear friction welding. Extended abstract, 8th Vienna International Conference on Mathematical Modelling, 2015.

[23] Jan Mikusiński and Thomas K. Boehme. *Operational Calculus*, volume I. Pergamon Press, Warsaw, 1987.

[24] Jan Mikusiński and Thomas K. Boehme. *Operational Calculus*, volume II. Pergamon Press, Warsaw, 1987.